Dissertation

GHS-R1a deficiency mitigates lipopolysaccharide-induced lung injury in mice via the downregulation of macrophage activity

The Graduate School of Advanced Preventive Medical Sciences

Supervisor: Prof. Toshinari TAKAMURA
*Research Field: Endocrinology and metabolism

Student ID: 2025012006

Ryota TANIDA

Contents

Dedication 4

Abstract 5

1. Introduction 6

2. Materials and Methods 8

2.1. Animals 8

2.2. LPS-induced lung injury 8

2.3. Plasma ghrelin determination 8

2.4. Histology 9

2.5. Murine bronchoalveolar lavage (BAL) experiment 9

2.6. Measurement of arterial oxygen saturation 9

2.7. Quantitative real-time PCR 9

2.8. Western blotting 10

2.9. Enzyme-linked immunosorbent assay (ELISA) 10

2.10. Isolation of mouse peritoneal macrophage 10

2.11. Mitochondrial respiration assays 11

2.12. Statistical analyses 11

3. Results 12

3.1. *Ghsr*$^{-/-}$ mice showed strong resistance to LPS-induced lung injury 12

3.2. Determination of experimental time course 13

3.3. **Ghrelin production in the stomach and plasma ghrelin levels after LPS administration** **14**

3.4. ***GHS-R1a*** **deficiency ameliorated lung inflammation and disruption of the alveolar barrier after LPS-induced lung injury** **15**

3.5. **Muted firing of inflammatory responses in** ***ghsr*** $^{-/-}$ **mice after lung injury** **17**

3.6. **Loss of GHS-R1a signal altered cytokine expression and inflammatory signaling activity in macrophages** **19**

3.7. ***GHS-R1a*** **deficiency lowers LPS-induced mitochondrial respiration** **21**

4. Discussion **24**

Acknowledgements **28**

References **29**

Dedication

I dedicate this work first to my ever-supporting family. To my family for all their support and encouragement in the moments I needed most. Moreover, they never allowed me to give up on this journey and have constantly been pushing me to reach the goal I am dreaming of. I would like to thank all my friends who always helped me when I needed the most for their words, advice, and support during this work. Without their help, I would not be here today. Again, I would like to say thank you to all those who helped my Ph.D. research life.

GHS-R1a deficiency mitigates lipopolysaccharide-induced lung injury in mice via the downregulation of macrophage activity

by

Ryota Tanida

Abstract

Acute respiratory distress syndrome (ARDS) is a critical illness syndrome characterized by dysregulated pulmonary inflammation. Currently, effective pharmacological treatments for ARDS are unavailable. Ghrelin, an endogenous ligand for the growth hormone secretagogue receptor type 1a (GHS-R1a), has a pivotal role in regulating energy metabolism and immunomodulation. The role of endogenous ghrelin in ARDS remains unclear. Herein, I investigated the role of endogenous ghrelin signaling by using GHS-R1a-null (*ghsr*$^{-/-}$) mice and lipopolysaccharide (LPS)-induced ARDS model. *Ghsr*$^{-/-}$ mice survived longer than controls after LPS-induced lung injury. *Ghsr*$^{-/-}$ mice showed lower levels of pro-inflammatory cytokines and higher oxygenation levels after lung injury. The peritoneal macrophages isolated from *ghsr*$^{-/-}$ mice exhibited lower levels of cytokines production and oxygen consumption rate after LPS stimulation. My results indicated that endogenous ghrelin plays a pivotal role in initiation and continuation of acute inflammatory response in the LPS-induced ARDS model by modulating macrophage activity, and highlighted endogenous GHS-R1a signaling in macrophage as a potential therapeutic target in this relentless disease.

Chapter 1

Introduction

Acute respiratory distress syndrome (ARDS) is a critical illness characterized by excessive acute inflammatory responses in lung parenchyma complicated with severe arterial hypoxia[1]. Excessive lung inflammation response greatly affects mortality in patients with ARDS[2]. Dysregulated lung inflammation leads to alveolar-capillary barrier disruption[3], which results in an excessive influx of neutrophils and macrophages in the alveoli and the development of fibrotic scarring.

In the initial phase of ARDS, macrophages have pivotal roles in initiating and maintaining the inflammatory response[4]. Macrophages recognize pathogen-associated molecular patterns (e.g. lipopolysaccharide (LPS)) through plasma membrane-anchored receptors such as toll-like receptors (TLRs). The binding of pattern recognition receptors (PRRs) activates the nuclear factor (NF)-κB pathway, which leads to a robust immune response via the induction of pro-inflammatory cytokines such as tumor necrosis factor-alpha (TNF-α), interleukin-1beta (IL-1β), and IL-6. Increased level of pro-inflammatory cytokines evokes alveolar-capillary barrier disruption, alveolar flooding, and alveolar infiltration of neutrophils[5].

Ghrelin is a 28-amino-acid peptide discovered as an endogenous ligand of growth hormone secretagogue receptor type 1a (GHS-R1a)[6]. In addition to its stimulatory action on growth hormone release, ghrelin is known to have multifactorial effects on the stimulation of food intake, provoking adiposity and the modulation of various immune responses[7]. Regarding ghrelin’s anti-inflammatory effects on lung inflammation, ghrelin administration mitigated lung edema, neutrophil infiltration, and

inflammatory cytokine levels by inhibiting the NF-κB pathway in a rat model of hemorrhagic shock-induced acute lung injury[8]. Conversely, in mice with dextran sulphate sodium (DSS)-induced colitis, the GHS-R1a deletion lowered pro-inflammatory cytokine production, macrophage infiltration, and TLR4 expression[9]. These findings led me to hypothesize that the role of endogenous ghrelin in the inflammatory mechanism of ARDS would differ from that of exogenous ghrelin treatment.

Here, I studied the role of endogenous ghrelin in the switching and expanding inflammatory responses by using a murine model of LPS-induced lung injury. My results revealed that an endogenous ghrelin signal is essential in initiating proper immune reaction after lung injury by modulating macrophage mitochondrial respiration.

Chapter 2

Materials and Methods

2.1. Animals

Control (C57BL/6J) mice bred in my laboratory were used. The *ghsr*$^{-/-}$ mice were kindly provided by Dr. Roy G. Smith (Baylor College of Medicine, TX, USA). In all experiments, we used 8- or 9-week-old mice (22–28 g). Both the C57BL/6J and *ghsr*$^{-/-}$ mice were maintained under a constant light-dark cycle (light on at 8:00 and off at 20:00) and temperature (23 ± 1°C). Water and standard laboratory chow were available *ad libitum*. All procedures strictly follow the Animal Care and Use Committee of Miyazaki University.

2.2. LPS-induced Lung Injury

Mice were anesthetized by an intraperitoneal injection of a mixture of three anesthetics: medetomidine hydrochloride (0.3 mg/kg), midazolam (4 mg/kg), and butorphanol tartrate (5 mg/kg). Mice were intratracheally (i.t.) injected 5 mg/kg or 10 mg/kg of LPS (*E. coli* O55:B5; Sigma-Aldrich, St. Louis, MO).

2.3. Plasma Ghrelin Determination

Samples for the ghrelin analysis were collected as we have described[10]. Plasma ghrelin concentration was measured with an AIA-600 II immunoassay analyzer (Tosoh, Tokyo).

2.4. Histology

The lungs and stomachs were fixed in 4% paraformaldehyde phosphate buffer solution (FUJIFILM Wako, Osaka, Japan) at 4°C overnight and then embedded in an OCT compound. Lung sections (4 μm) and stomach sections (6 μm) were mounted on the slides and stained for hematoxylin and eosin (H&E) or immunostaining with an antibody recognizing ghrelin (sc-517596, Santa Cruz Biotechnology, CA).

2.5. Murine Bronchoalveolar Lavage (BAL) Experiment

At 24 hours after the LPS installation, mice were subjected to bronchoalveolar lavage (BAL) experiments as previously described[10]. The BAL fluid (BALF) from each animal was centrifuged at 1,000 rpm for 5 min, and the supernatant was stored at −80°C until assay. Cell differentials were determined by Diff-Quick staining. Alveolar barrier permeability was determined by measurement of total protein in the BALF supernatant measured by Bradford assay.

2.6. Measurement of Arterial Oxygen Saturation

I collected blood samples from the left ventricle of the anesthetized mouse. The partial pressure of arterial oxygen (PaO_2) levels were measured by a blood gas analyzer (ABL9, Radiometer, Tokyo) according to the manufacturer's instructions. The PaO_2/fraction of inspiratory oxygen (FiO_2) ratio was calculated while the mice breathed room air ($FiO_2 = 0.21$).

2.7. Quantitative Real-time PCR

The total RNA of mouse lungs and isolated peritoneal macrophages was extracted using TRIzol reagent (Invitrogen, Carlsbad, CA). First-strand complementary

DNA was synthesized using a High-Capacity RNA-to-cDNA kit (Applied Biosystems, Foster City, CA). I used TaqMan Fast Universal PCR Master Mix (Thermo Fisher Scientific, Waltham, MA) and a Thermal Cycler Dice Real-Time System II (Takara Bio, Shiga, Japan) to detect the gene expression and calculated it by the ΔΔCT method. The used primers are as follows: *Il-6*, Mm00446190_m1; *Tnf-α*, Mm00443258_m1, C-C motif chemokine2 (*Ccl2*), Mm00441242_m1, chemokine (C-X-C motif) ligand 2/macrophage inhibitory protein-2 (*Cxcl2/MIP2*), Mm00436450_m1; and *Gapdh* (glyceraldehyde 3-phosphate dehydrogenase), Mm99999915_g1.

2.8. Western Blotting

I conducted western blotting using antibodies recognizing the following proteins: TGF-beta-activated kinase 1 and MAP3K7-binding protein 2 (TAB2), IκB, NF-κB (Cell Signaling Technology, Danvers, MA), and β-actin (Sigma-Aldrich Japan, Tokyo). The protein expression was quantified by densitometry using Fusion FX software (Vilber Lourmat, Collégien, France).

2.9. Enzyme-linked Immunosorbent Assay (ELISA)

The concentrations of IL-6, TNF-α, IL-1β, CCL2 and CXCL2/MIP2 in the BALF were determined by the respective mouse ELISA kits (R&D Systems, Minneapolis, MN).

2.10. Isolation of Mouse Peritoneal Macrophage

I sacrificed mice and injected 5 ml of phosphate-buffered saline (PBS) that contained 3% fetal bovine serum (FBS) into the peritoneal cavity. I then collected the peritoneal cavity cells using an 18-ga. needle. The red blood cells were lysed using

ACK lysis buffer (Lonza, Walkersville, MD) after centrifugation at 1,000 rpm for 3 min. Isolated cells were seeded with a proper cell number for each experiment and cultured with RPMI-1640 medium at 37℃ in a CO_2 incubator.

2.11. Mitochondrial Respiration Assays

I monitored the real-time oxygen consumption rate (OCR) and the extracellular acidification rate (ECAR) in mouse peritoneal macrophages by using XFp Analyzer (Agilent Technologies, Santa Clara, CA) according to the manufacturer's instruction.

2.12. Statistical Analyses

All statistical analyses were performed using GraphPad PRISM 9 software (Graph Pad Software, La Jolla, CA). The data were analyzed by a one-way or two-way analysis of variance (ANOVA) followed by the Tukey-Kramer method for multiple comparisons. I conducted a Kaplan-Meier analysis for the survival data. All data are expressed as the mean ± standard error of the mean (SEM). Probability (*P*)-values < 0.05 were considered significant.

Chapter 3

Results

3.1. *Ghsr*$^{-/-}$ mice showed strong resistance to LPS-induced lung injury

To determine the significance of endogenous GHS-R1a expression in acute lung injury, I intratracheally injected LPS into *ghsr*$^{-/-}$ mice. Surprisingly, *ghsr*$^{-/-}$ mice survived significantly longer than the control mice after LPS administration (Figure 1). The survival rates of the *ghsr*$^{-/-}$ mice and control mice at 72 hours after LPS administration were 92.3% and 23%, respectively.

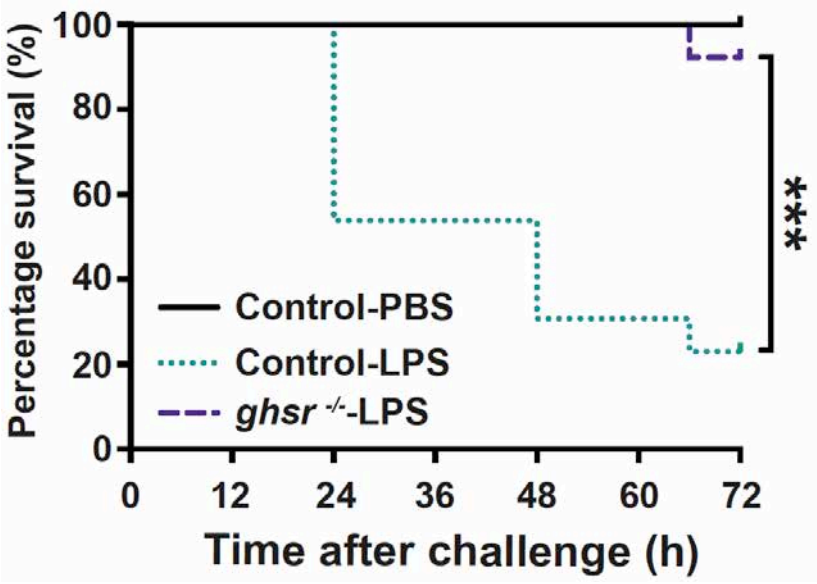

Figure 1: ***The survival rate after LPS-induced lung injury.*** Kaplan-Meier survival curves at 72 hours after the challenge with 10 mg/kg of LPS or PBS under ad libitum feeding (n = 13 per group).Values are mean ± SEM. *** $P < 0.001$.

3.2. Determination of experimental time course

I confirmed the *Il-6* mRNA expression levels in the mice's lungs after LPS administration at 0, 1, 3, 6, and 24 hours to determine a proper time point for my study hereafter. The *Il-6* mRNA expression levels gradually increased and peaked at 24 hours, but a significant increase was not observed in *ghsr*$^{-/-}$ mice (Figure 2). The mice's food intake and body weight were comparable in both genotypes at 24 hours (Figure 3A and B). Given these results, I selected 24 hours as the analysis time point.

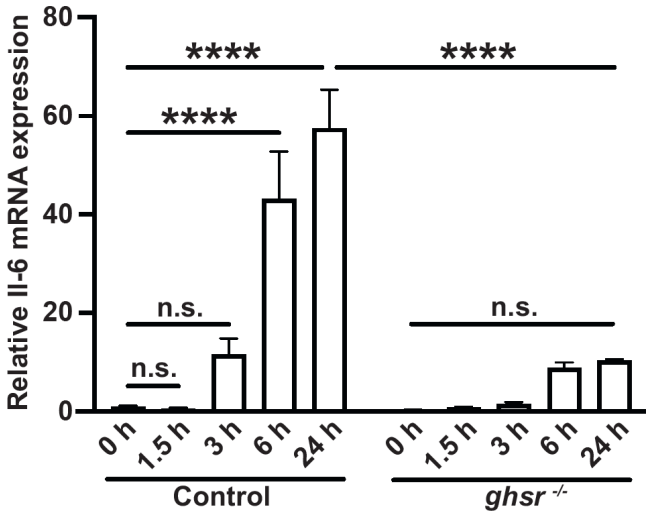

Figure 2: ***The alteration of Il-6 mRNA expression levels in the lungs at different time point after LPS administration.*** The mice were received i.t. administration of 5 mg/kg of LPS or PBS (n = 3 per group). Values are mean ± SEM. **** $P < 0.0001$, n.s. not significant.

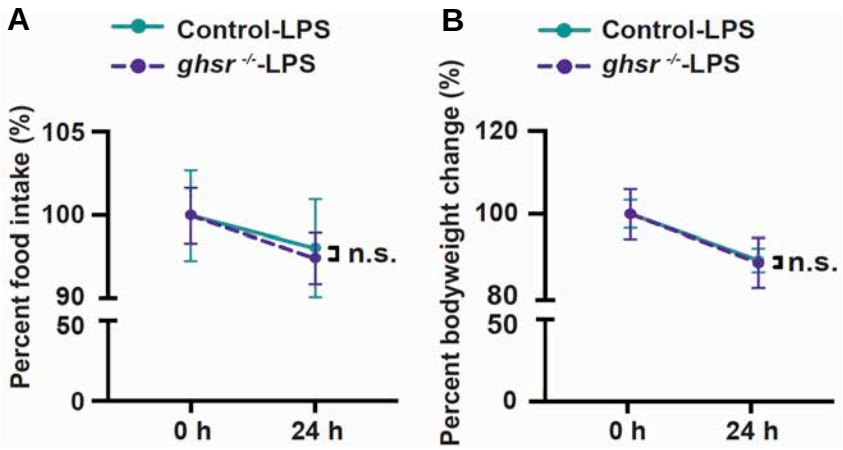

Figure 3: ***Alteration in the food intake amount and body weight.*** (A) The food intake, (B) body weight changes with LPS administration of 5 mg/kg of LPS (Control-LPS: n = 5; *ghsr*$^{-/-}$-LPS: n = 6). Values are mean ± SEM, n.s. not significant.

3.3. Ghrelin production in the stomach and plasma ghrelin levels after LPS administration

I confirmed endogenous ghrelin production and serum levels 24 hours after LPS administration. As Figure 4 shows, LPS administration significantly reduced the number of ghrelin-positive cells in the stomach tissues of control mice. Although the LPS administration significantly reduced the plasma ghrelin levels in both genotypes, declining levels were lower in the *ghsr*$^{-/-}$ mice (Figure 5).

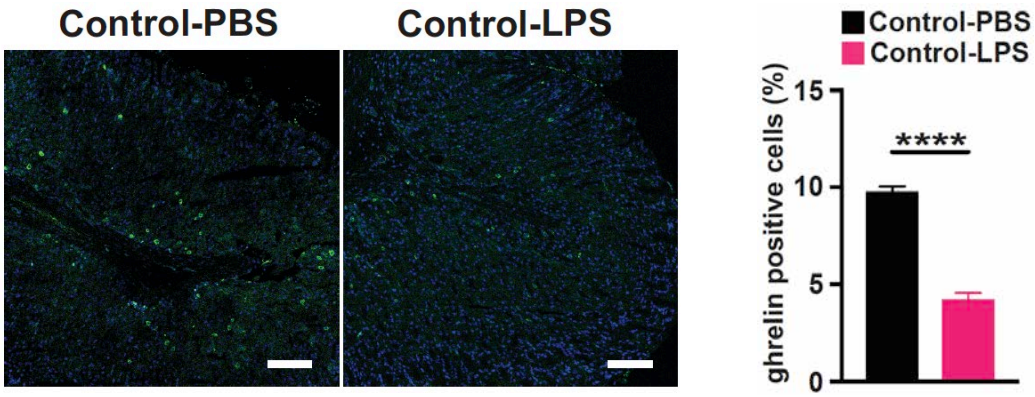

Figure 4: ***Ghrelin production in the stomach after LPS administration.*** Representative profiles of ghrelin immunohistostaining (green) from 4 mice per group. 4', 6'-diamino-2-phenylindole (DAPI) was used in the counterstaining of the nucleus (blue). Scale bar, 100 μm. Values are mean ± SEM. **** $P < 0.0001$.

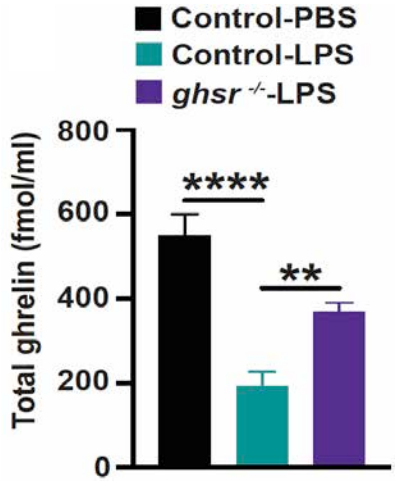

Figure 5: ***Plasma ghrelin concentration after LPS administration.*** Plasma ghrelin concentration at 24 hours after the administration of 5 mg/kg of LPS or PBS (Control-PBS, n = 5; Control-LPS, n = 6; *ghsr*$^{-/-}$-LPS, n = 6). Values are mean ± SEM. ** $P < 0.01$ **** $P < 0.0001$

3.4. *GHS-R1a* deficiency ameliorated lung inflammation and disruption of the alveolar barrier after LPS-induced lung injury

I next assessed the influence of *GHS-R1a* deficiency on inflammatory cell infiltration and lung vascular permeability after lung injury. The BALF collected from LPS-administered control mice showed dark pink, indicating rich protein content in the BALF caused by disruption of alveolar barrier integrity after injury. In contrast, the BALF of the *ghsr*$^{-/-}$ mice was almost transparent (Figure 6A). The protein level in the BALF of *ghsr*$^{-/-}$ mice was significantly lower than that of control mice (Figure 6B).

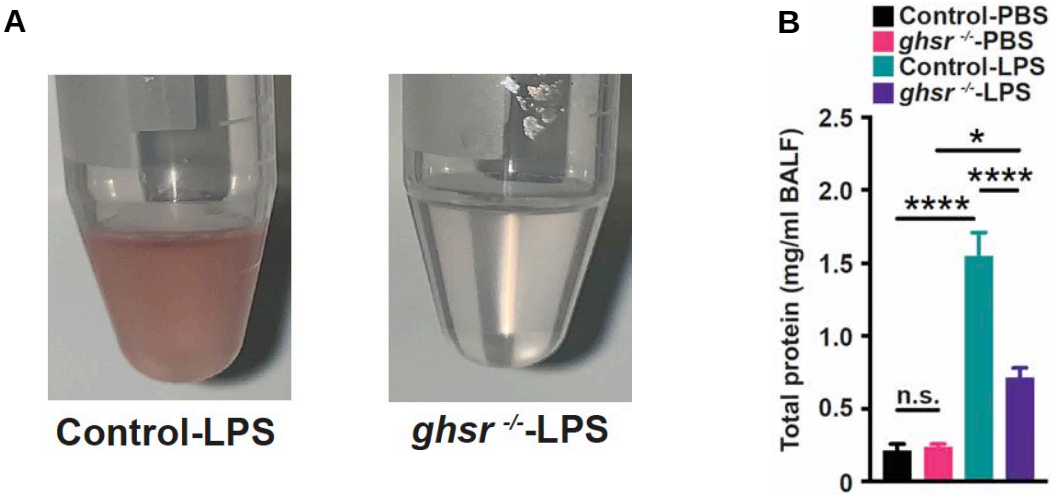

Figure 6: ***The BALF samples from the LPS-administered mice.*** (A) Photographs of the BALF collected 24 hours after LPS administration (representative BALF from 8 mice per group). (B) Total protein concentration (Control-PBS, n = 8; *ghsr*$^{-/-}$-PBS, n = 8; Control-LPS, n = 14; *ghsr*$^{-/-}$-LPS, n = 14) in the BALF of control and *ghsr*$^{-/-}$ mice. Values are mean ± SEM. * $P < 0.05$, **** $P < 0.0001$, n.s. not significant.

Histologically, the lungs of the *ghsr*$^{-/-}$ mice showed minor degree of interalveolar edema after lung injury (Figure 7A). Although the numbers of total cells and neutrophils infiltrated into the alveoli were similar in both genotypes, the macrophage numbers in the BALF of *ghsr*$^{-/-}$ mice were significantly lower than those of control mice (Figure 7B). The PaO_2/FiO_2 ratio of LPS-administered control mice was significantly lower than PBS-administered control mice (Figure 8). This PaO_2/FiO_2 ratio value in the LPS-

injected control mice corresponds to moderate ARDS in humans[11]. The oxygenation level in LPS-administered *ghsr*$^{-/-}$ mice was significantly higher than the counterpart of control mice, and comparable to that of PBS-injected *ghsr*$^{-/-}$ mice.

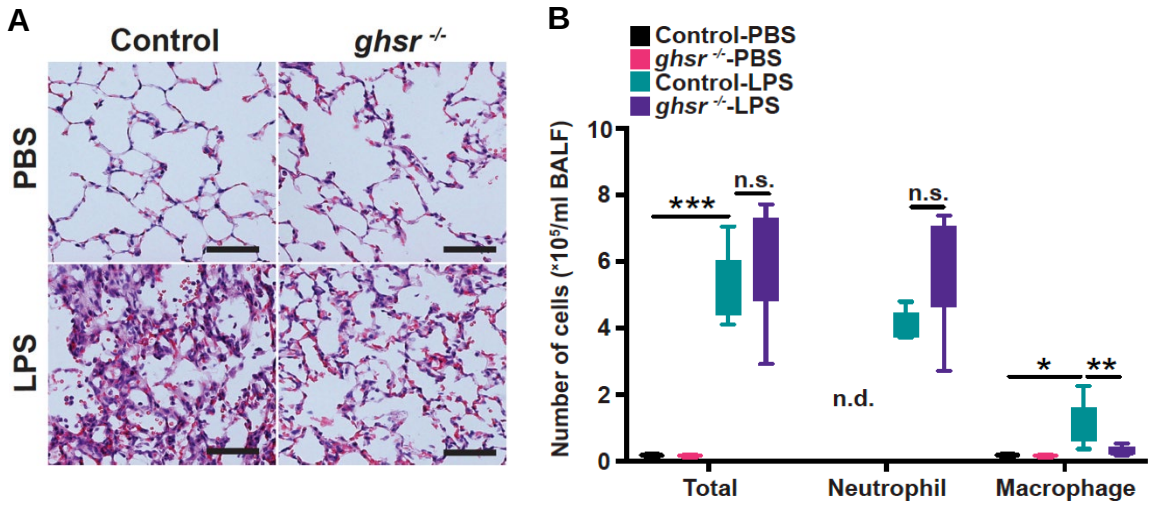

Figure 7: ***Lung morphological change and immune cell infiltration after LPS administration.*** (A) Hematoxylin-eosin (HE) staining of lung sections from control mice (*left panels*) and *ghsr*$^{-/-}$ (*right panels*) mice after the administration of PBS (*upper panels*) or 5 mg/kg of LPS (*lower panels*). The data are representative lung sections from 6 mice per group. (scale bar: 50 μm). (B) Cell counts (Control-PBS, n = 3; *ghsr*$^{-/-}$-PBS, n = 3; Control-LPS, n = 7; *ghsr*$^{-/-}$-LPS, n = 7) in the BALF of control and *ghsr*$^{-/-}$ mice. Values are mean ± SEM. * $P < 0.05$, ** $P < 0.01$, *** $P < 0.001$, n.s. not significant, n.d. not detected.

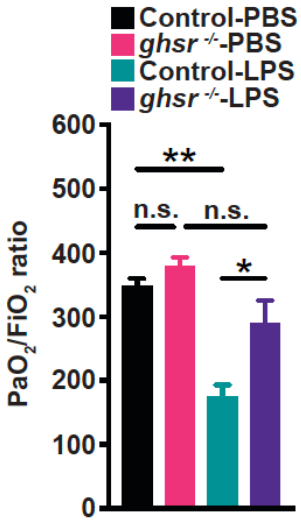

Figure 8: ***The oxygenation level after LPS administration.*** A blood gas analysis was conducted 24 hours after LPS administration to determine the ratio of partial pressure (PaO_2) to fractional inspired oxygen (FiO_2) (Control-PBS, n = 3; *ghsr*$^{-/-}$-PBS, n = 3; Control-LPS, n = 4; *ghsr*$^{-/-}$-LPS, n = 4). Values are mean ± SEM. * $P < 0.05$, ** $P < 0.01$, n.s. not significant.

3.5. Muted firing of inflammatory responses in *ghsr*$^{-/-}$ mice after lung injury

The increase in the pNF-κB/NF-κB ratio of the *ghsr*$^{-/-}$ mice was significantly lower than that of the control mice after LPS administration. The IκB protein levels increased in the lungs of control mice, whereas the counterpart of *ghsr*$^{-/-}$ mice was not changed after lung injury (Figure 9). A previous report applying mathematical modeling of NF-κB signaling revealed that upregulation of IκB occurs as negative feedback for NF-κB[12]. In LPS-administered mice, IL-6, TNF-α, IL-1β, and CCL2 values were significantly lower in the *ghsr*$^{-/-}$ mice compared to the control (Figure 10).

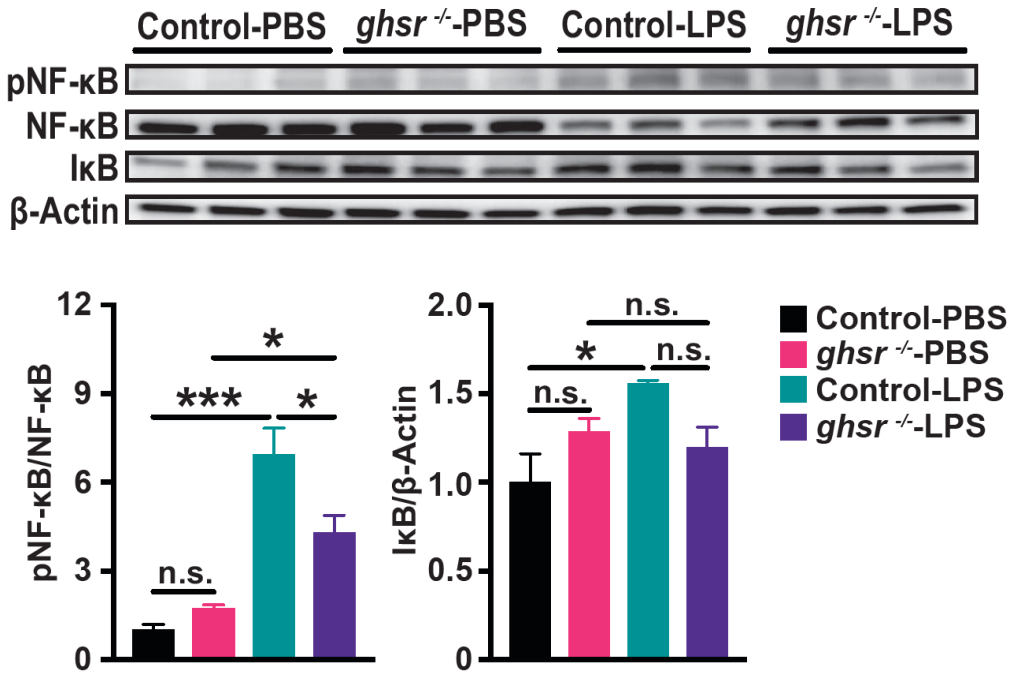

Figure 9: ***NF-κB signaling activity in the lungs after LPS administration.*** Immunoblots of the NF-κB and IκB protein levels in the lysates of whole lung tissue from 5 mg/kg LPS- or PBS-injected mice. The quantitative comparisons were performed by using total NF-κB and β-actin as loading controls, respectively (n = 3 per group). Values are mean ± SEM. * $P < 0.05$, *** $P < 0.001$, n.s. not significant.

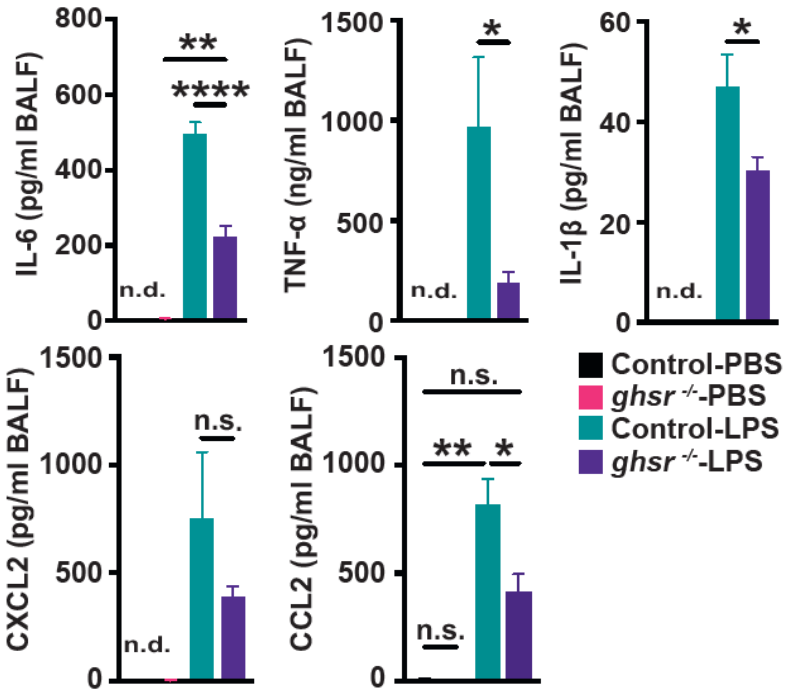

Figure 10: ***The cytokine levels in the BALF.*** Concentration of IL-6, TNF-α, IL-1β, CXCL2, and CCL2 protein in the BALF (Control-PBS, n = 3; *ghsr*$^{-/-}$-PBS, n = 3; Control-LPS, n = 7; *ghsr*$^{-/-}$-LPS, n = 7). Values are mean ± SEM. * $P < 0.05$, ** $P < 0.01$, **** $P < 0.0001$, n.s. not significant, n.d. not detected.

3.6. Loss of GHS-R1a signal altered cytokine expression and inflammatory signaling activity in macrophages

The immune response triggered by macrophage activation plays a pivotal role in the initial phase of ARDS[4]. I, therefore, focused on the role of GHS-R1a signaling in macrophages under LPS stimulation.

The mRNA levels of pro-inflammatory cytokines and chemokines were elevated in the LPS-stimulated isolated macrophages. Among the LPS-stimulated macrophage, induction levels of cytokines and chemokines were suppressed in *ghsr*$^{-/-}$ mice. The *Il-10* mRNA levels were higher in *ghsr*$^{-/-}$ mice compared to the control mice (Figure 11).

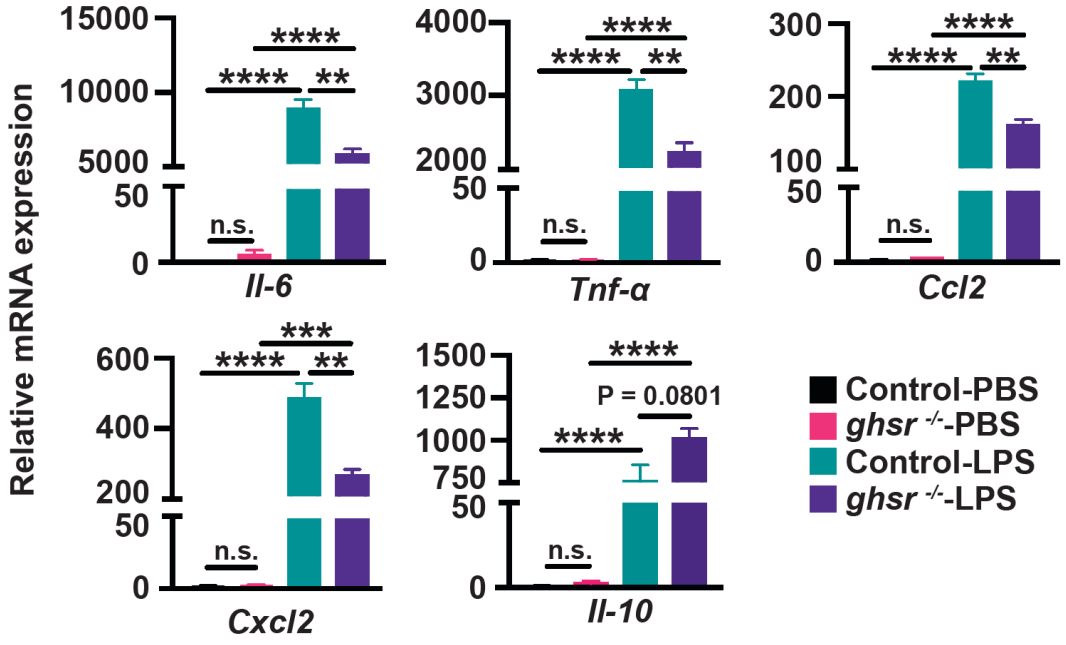

Figure 11: ***The cytokine expression levels in macrophages after LPS stimulation.*** Relative mRNA expression levels of *Il-6*, *Tnf-α*, *Il-1β*, *Ccl2*, *Cxcl2*, and *Il-10* in peritoneal macrophage cells at 2 hours after LPS stimulation. Gene expressions were normalized with *Gapdh* (n = 3, per group). Values are mean ± SEM. ** $P < 0.01$, **** $P < 0.0001$, n.s. not significant.

Moreover, [D-Lys3]-GHRP6, a GHS-R1a antagonist, treatment suppressed the activation of TAB2 and NF-κB in isolated macrophages from control mice (Figure 12).

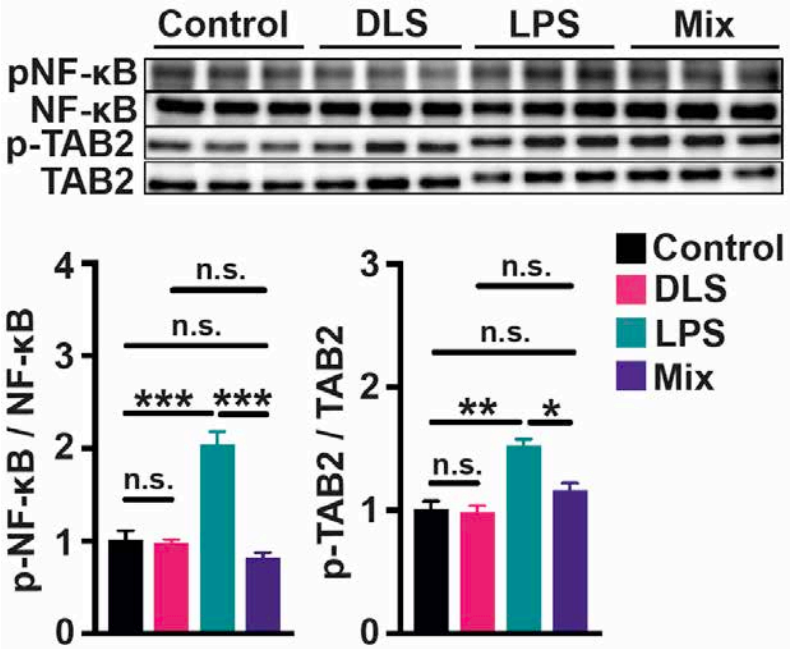

Figure 12: ***Inflammatory signals in macrophages after LPS stimulation.*** Immunoblots of the pNF-κB/NF-κB and pTAB2/TAB2 ratio in peritoneal macrophage (n = 3 per group). The macrophages were pretreated with GHS-R1a inhibitor (DLS, 100nM) for 1 hour and then treated with LPS (1μg/ml) for 30 min. DLS = [D-Lys3]-GHRP6; Mix = DLS-LPS. Values are mean ± SEM. * $P < 0.05$, ** $P < 0.01$, *** $P < 0.001$, n.s. not significant.

3.7. *GHS-R1a* deficiency lowers LPS-induced mitochondrial respiration

LPS-activated macrophages are known to convert the tricarboxylic acid cycle into the glycolytic pathway as an energy source to sustain the cells' high secretory and phagocytic functions[13]. To investigate the mitochondrial bioenergetic change in LPS-stimulated macrophages, I measured the OCR sequentially, an indicator of mitochondrial respiration.

In unstimulated peritoneal macrophages, the parameters of the OCR were comparable between the two genotypes. In contrast, the macrophages isolated from *ghsr*$^{-/-}$ mice showed a drastic reduction of mitochondrial respiration and ATP production after LPS stimulation (Figure 13).

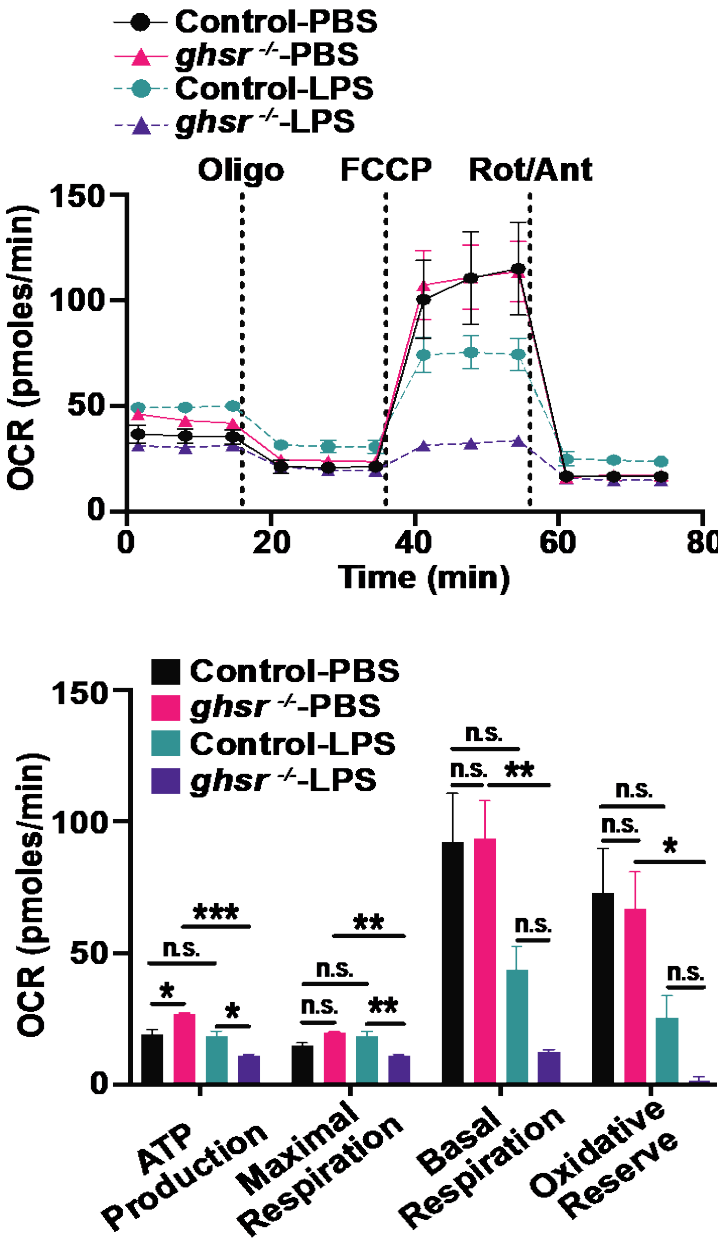

Figure 13: ***OCR alteration in macrophages after LPS stimulation.*** The real-time oxygen consumption rate (OCR) in peritoneal macrophage cells at 2 hours after LPS stimulation (n=3 per group). The LPS concentration was 1 µg/ml in all peritoneal macrophage experiments. The mitochondrial stress test was assessed by recording OCR after injection of oligomycin (Oligo, 1 µM), carbonyl cyanide-4-(trifluoromethoxy), phenylhydrazone (FCCP, 0.7 µM), and rotenone (ROT, 1 µM) plus antimycin (Ant, 1 µM). Values are mean ± SEM. *p<0.05, **p<0.01, ***p<0.001, n.s. not significant.

The macrophages isolated from *ghsr*$^{-/-}$ mice also showed decreased glycolytic capacity after LPS stimulation (Figure 14). These data indicated that the endogenous GHS-R1a signal has a pivotal role in maintaining LPS-induced mitochondrial metabolic reprogramming.

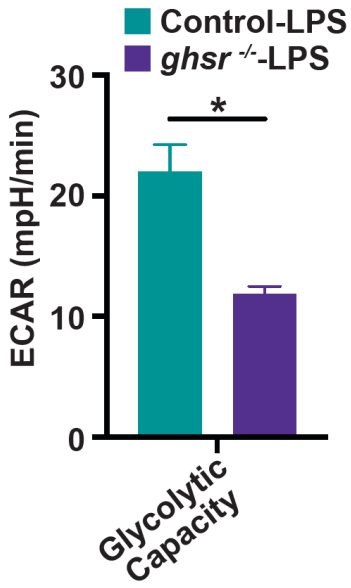

Figure 14: ***Glycolytic capacity in macrophages after LPS stimulation.*** The real-time extracellular acidification rate (ECAR) in peritoneal macrophage cells at 2 hours after LPS stimulation (n=3 per group). The LPS concentration was 1 μg/ml in all peritoneal macrophage experiments. The mitochondrial stress test was assessed by recording ECAR after injection of oligomycin (Oligo, 1 μM), carbonyl cyanide-4-(trifluoromethoxy), phenylhydrazone (FCCP, 0.7 μM), and rotenone (ROT, 1 μM) plus antimycin (Ant, 1 μM). Values are mean ± SEM. *p<0.05.

Chapter 4

Discussion

Uncontrolled systemic inflammatory response occurring during the course of ARDS is closely associated with an infiltration of inflammatory cells into the lungs, an excessive release of pro-inflammatory cytokines, and subsequent parenchymal damage. However, anti-inflammatory approaches, including corticosteroids, have not shown clinical efficacy as treatments in patients with ARDS[1]. In the present study, I explored the influence of the deletion of ghrelin~GHS-R1a signaling on LPS-induced lung injury. The null mutation of *GHS-R1a* significantly improved the survival rate associated with alleviated lung inflammation and protected alveolar barrier integrity in LPS-treated mice. *GHS-R1a* deficiency specifically blocked macrophage accumulation in the lungs after LPS administration. Notably, macrophages lacking *GHS-R1a* exhibited reduced expressions of pro-inflammatory cytokines and production of mitochondrial ATP. My results indicated that deletion of GHS-R1a signaling, especially macrophage-specific antagonism, may be a potential therapeutic target for ARDS.

I demonstrated that *GHS-R1a*-knockout mice are protected from LPS-induced lung injury. My finding is consistent with prior studies demonstrating the mitigation of DSS-induced colitis and high-fructose corn syrup-induced adipose inflammation in *GHS-R1a*-deficient mice[9,14]. *GHS-R1a*-knockout mice showed a lower disease severity index, lower inflammatory cytokine production, and less macrophage infiltration in DSS-induced colitis. The levels of IL-6 and TNF-α released from LPS-stimulated peritoneal macrophages of *GHS-R1a*-knockout mice are significantly lower than those of wild-type mice[9]. *GHS-R1a* knockdown in a macrophage cell line

suppressed LPS-induced pro-inflammatory cytokine expression[14]. In contrast, in several injury models, exogenous ghrelin administration protects from excessive inflammation and tissue damage, including LPS-induced lung injury[15,16].

Regarding the opposite result observed between endogenous GHS-R1a-ablated condition and exogenous ghrelin treatment against LPS-induced inflammation, we focused on the role of GHS-R1a in macrophage mitochondrial bioenergetic function. Exogenous ghrelin treatment activates mitochondrial function, including mitochondrial respiration[17,18]. On the other hand, it is known that mitochondrial respiration declined in skeletal muscles in *GHS-R1a*-knockout mice[19]. Activated macrophages stimulated by LPS run metabolic reprogramming from oxidative phosphorylation to glycolysis, producing pro-inflammatory cytokines efficiently[13]. The reprogramming of cellular metabolism is a beneficial response to generate ATP rapidly. The cellular metabolic reprogramming is vital for the generation of redox equivalents as well as precursor molecules such as amino acids, lipids, and nucleotides, sustaining a burst in pro-inflammatory mediator production[13,20]. My present results demonstrated that the glycolytic capacity of the macrophages and ATP level isolated from *ghsr*$^{-/-}$ mice were significantly lower than those of the control mice. The suppressed glycolytic capacity would reflect the blockade of a metabolic pathway shift from oxidative phosphorylation to aerobic glycolysis, which may contribute to the suppression of lung inflammation in *ghsr*$^{-/-}$ mice.

I showed that *GHS-R1a* deletion significantly suppressed the NF-κB pathway activity and induction of pro-inflammatory cytokines in the lungs after LPS injection. I also showed that GHS-R1a antagonism abrogated LPS-induced NF-κB activation in isolated macrophages. Since NF-κB signaling is a master regulator of pro-inflammatory

cytokine induction, GHS-R1a inhibition might mitigate lung inflammation via downregulation of NF-κB activation in macrophage.

In this study, I did not reveal whether GHS-R1a expression directly or indirectly modulates TLR4 signaling activity. GHS-R1a is known to form heterodimers with other GPCRs, including somatostatin receptor subtype 5, dopamine receptor subtype 1, and serotonin 2C receptor[21]. The heterodimerized GHS-R1a regulates signal transduction of the linked GPCR in the absence of ghrelin[21]. In the present study, I showed NF-κB activation after LPS stimulation was suppressed in both isolated macrophages from *ghsr*$^{-/-}$ mice and GHS-R1a antagonist treatment in wild-type mice. Future studies are required to clarify whether GHS-R1a influences the signal transduction of PRRs, including TLR4.

There are some important limitations to address in this study. It is unclear whether GHS-R1a ablation in macrophages preferentially mitigates LPS-induced lung inflammation. GHS-R1a is expressed in various cells other than macrophages, including T lymphocytes, neutrophils and alveolar epithelial cells[22,23]. In this study, I present two lines of data suggesting that loss of GHS-R1a expression in macrophages plays a major role in mitigating LPS-induced lung inflammation. First, in the isolated macrophages, GHS-R1a blockage suppressed the pro-inflammatory cytokine induction and NF-κB activation after LPS stimulation, similar to what was seen in whole lung tissue in *ghsr*$^{-/-}$ mice. Second, in *ghsr*$^{-/-}$ mice, the accumulation of macrophages in the lungs was selectively suppressed after LPS administration. These data suggest that the GHS-R1a inhibition in macrophages contributes to mitigating LPS-induced lung inflammation.

I obtained differing results regarding the *Cxcl2* expression level due to *GHS-R1a* deficiency between whole lung tissue of LPS-injected mice and LPS-stimulated

macrophages. In the entire lung tissue, *GHS-R1a* deficiency did not affect *Cxcl2* expression in LPS-administered mice. However, in the macrophages, loss of GHS-R1a signaling resulted in a decreased expression of *Cxcl2*. CXCL2 is produced downstream of TLRs in both macrophages and neutrophils in response to a wide range of bacterial pathogens[24]. In the present study, the number of macrophages that infiltrated the alveolar space was suppressed in *ghsr*$^{-/-}$ mice compared to control mice, whereas the number of neutrophils was similar between the two genotypes. These data indicated that the influence of *GHS-R1a* deficiency on cellular functions, such as infiltration and cytokine production, may differ between macrophages and neutrophils.

In conclusion, the present study demonstrated that *GHS-R1a* deficiency effectively reduced lung inflammation, maintained respiratory status, and improved the survival rate in LPS-injected mice. The underlying mechanisms of these phenomena can be expected to be related to impaired production activity of inflammatory cytokines in macrophages. My findings indicate that GHS-R1a inhibitors specific to macrophages may be a promising candidate for treating ARDS.

Acknowledgements

I would like to express my appreciation to all those who have made my Ph.D. possible. First, thank my supervisor, Dr. Toshinari Takamura, my principal advisor, Dr. Hironobu Tsubouchi, Dr. Shigehisa Yanagi, and Dr. Koji Toshinai for encouraging me to give my best during my Ph.D. program. To Dr. Masmitsu Nakazato and Dr. Taiga Miyazaki for providing and supporting me to use the facilities and their funds. To Dr. Yusuke Saito, thank you for letting me use the XFp Analyzer facilities to implement my experiments and for providing several tips to promote my study. Thank you for your technical support to Ms. Sumie Tajiri, Ms. Eiko Kurata, and Ms. Itsuki Morinaga. To the University of Miyazaki for allowing me to use the laboratories to cultivate my research experience. I would like to thank Kanazawa University, WISE Program for Nano-Precision Medicine, Science, and Technology of Kanazawa University by MEXT and JST for their constant support in paying my tuition and the living help that allowed me to acquire the Ph.D. degree.

References

[1] L.A. Huppert, M.A. Matthay, L.B. Ware, Pathogenesis of Acute Respiratory Distress Syndrome, Semin Respir Crit Care Med. 40 (2019) 31–39. https://doi.org/10.1055/S-0039-1683996.

[2] Y. Imai, K. Kuba, G.G. Neely, R. Yaghubian-Malhami, T. Perkmann, G. van Loo, M. Ermolaeva, R. Veldhuizen, Y.H.C. Leung, H. Wang, H. Liu, Y. Sun, M. Pasparakis, M. Kopf, C. Mech, S. Bavari, J.S.M. Peiris, A.S. Slutsky, S. Akira, M. Hultqvist, R. Holmdahl, J. Nicholls, C. Jiang, C.J. Binder, J.M. Penninger, Identification of oxidative stress and Toll-like receptor 4 signaling as a key pathway of acute lung injury, Cell. 133 (2008) 235–249. https://doi.org/10.1016/J.CELL.2008.02.043.

[3] H.H. Ginzberg, P.T. Shannon, T. Suzuki, O. Hong, E. Vachon, T. Moraes, M.T.H. Abreu, V. Cherepanov, X. Wang, C.W. Chow, G.P. Downey, Leukocyte elastase induces epithelial apoptosis: role of mitochondial permeability changes and Akt, Am J Physiol Gastrointest Liver Physiol. 287 (2004). https://doi.org/10.1152/AJPGI.00350.2003.

[4] E.K.Y. Fan, J. Fan, Regulation of alveolar macrophage death in acute lung inflammation, Respir Res. 19 (2018). https://doi.org/10.1186/S12931-018-0756-5.

[5] B. Opitz, V. Van Laak, J. Eitel, N. Suttorp, Innate immune recognition in infectious and noninfectious diseases of the lung, Am J Respir Crit Care Med. 181 (2010) 1294–1309. https://doi.org/10.1164/RCCM.200909-1427SO.

[6] M. Kojima, H. Hosoda, Y. Date, M. Nakazato, H. Matsuo, K. Kangawa, Ghrelin is a growth-hormone-releasing acylated peptide from stomach, Nature. 402 (1999) 656–660. https://doi.org/10.1038/45230.

[7] M. Nakazato, N. Murakami, Y. Date, M. Kojima, H. Matsuo, K. Kangawa, S. Matsukura, A role for ghrelin in the central regulation of feeding, Nature. 409 (2001) 194–198. https://doi.org/10.1038/35051587.

[8] H. Zheng, W. Liang, W. He, C. Huang, Q. Chen, H. Yi, L. Long, Y. Deng, M. Zeng, Ghrelin attenuates sepsis-induced acute lung injury by inhibiting the NF-κB, iNOS, and Akt signaling in alveolar macrophages, Am J Physiol Lung Cell Mol Physiol. 317 (2019) L381–L391. https://doi.org/10.1152/AJPLUNG.00253.2018.

[9] Z.Z. Liu, W.G. Wang, Q. Li, M. Tang, J. Li, W.T. Wu, Y.H. Wan, Z.G. Wang, S.S. Bao, J. Fei, Growth hormone secretagogue receptor is important in the development of experimental colitis, Cell Biosci. 5 (2015). https://doi.org/10.1186/S13578-015-0002-5.

[10] H. Tsubouchi, S. Yanagi, A. Miura, S. Iizuka, S. Mogami, C. Yamada, T. Hattori, M. Nakazato, Rikkunshito ameliorates bleomycin-induced acute lung injury in a ghrelin-independent manner, Am J Physiol Lung Cell Mol Physiol. 306 (2014). https://doi.org/10.1152/AJPLUNG.00096.2013.

[11] N.D. Ferguson, E. Fan, L. Camporota, M. Antonelli, A. Anzueto, R. Beale, L. Brochard, R. Brower, A. Esteban, L. Gattinoni, A. Rhodes, A.S. Slutsky, J.L. Vincent, G.D. Rubenfeld, B. Taylor Thompson, V. Marco Ranieri, The Berlin definition of ARDS: an expanded rationale, justification, and supplementary material, Intensive Care Med. 38 (2012) 1573–1582. https://doi.org/10.1007/S00134-012-2682-1.

[12] R. Cheong, A. Hoffmann, A. Levchenko, Understanding NF-kappaB signaling via mathematical modeling, Mol Syst Biol. 4 (2008). https://doi.org/10.1038/MSB.2008.30.

[13] J. Van den Bossche, L.A. O'Neill, D. Menon, Macrophage Immunometabolism: Where Are We (Going)?, Trends Immunol. 38 (2017) 395–406. https://doi.org/10.1016/J.IT.2017.03.001.

[14] X. Ma, L. Lin, J. Yue, G. Pradhan, G. Qin, L.J. Minze, H. Wu, D. Sheikh-Hamad, C.W. Smith, Y. Sun, Ghrelin receptor regulates HFCS-induced adipose inflammation and insulin resistance, Nutr Diabetes. 3 (2013) e99–e99. https://doi.org/10.1038/NUTD.2013.41.

[15] Ghrelin attenuates lipopolysaccharide-induced acute lung injury through NO pathway - PubMed, (n.d.). https://pubmed.ncbi.nlm.nih.gov/18591913/ (accessed December 13, 2023).

[16] B. Li, M. Zeng, W. He, X. Huang, L. Luo, H. Zhang, D.Y.B. Deng, Ghrelin protects alveolar macrophages against lipopolysaccharide-induced apoptosis through growth hormone secretagogue receptor 1a-dependent c-Jun N-terminal kinase and Wnt/β-catenin signaling and suppresses lung inflammation, Endocrinology. 156 (2015) 203–217. https://doi.org/10.1210/EN.2014-1539.

[17] Z.B. Andrews, Z.W. Liu, N. Walllingford, D.M. Erion, E. Borok, J.M. Friedman, M.H. Tschöp, M. Shanabrough, G. Cline, G.I. Shulman, A. Coppola, X.B. Gao, T.L. Horvath, S. Diano, UCP2 mediates ghrelin's action on NPY/AgRP neurons by lowering free radicals, Nature. 454 (2008) 846–851. https://doi.org/10.1038/NATURE07181.

[18] C.S. Wu, Q. Wei, H. Wang, D.M. Kim, M. Balderas, G. Wu, J. Lawler, S. Safe, S. Guo, S. Devaraj, Z. Chen, Y. Sun, Protective Effects of Ghrelin on Fasting-

Induced Muscle Atrophy in Aging Mice, J Gerontol A Biol Sci Med Sci. 75 (2020) 621–630. https://doi.org/10.1093/GERONA/GLY256.

[19] H. Liu, P. Zang, I. Lee, B. Anderson, A. Christiani, L. Strait-Bodey, B.A. Breckheimer, M. Storie, A. Tewnion, K. Krumm, T. Li, B. Irwin, J.M. Garcia, Growth hormone secretagogue receptor-1a mediates ghrelin's effects on attenuating tumour-induced loss of muscle strength but not muscle mass, J Cachexia Sarcopenia Muscle. 12 (2021) 1280–1295. https://doi.org/10.1002/JCSM.12743.

[20] S.S. Im, L. Yousef, C. Blaschitz, J.Z. Liu, R.A. Edwards, S.G. Young, M. Raffatellu, T.F. Osborne, Linking lipid metabolism to the innate immune response in macrophages through sterol regulatory element binding protein-1a, Cell Metab. 13 (2011) 540–549. https://doi.org/10.1016/J.CMET.2011.04.001.

[21] S. Yanagi, T. Sato, K. Kangawa, M. Nakazato, The Homeostatic Force of Ghrelin, Cell Metab. 27 (2018) 786–804. https://doi.org/10.1016/J.CMET.2018.02.008.

[22] N. Hattori, T. Saito, T. Yagyu, B.H. Jiang, K. Kitagawa, C. Inagaki, GH, GH receptor, GH secretagogue receptor, and ghrelin expression in human T cells, B cells, and neutrophils, J Clin Endocrinol Metab. 86 (2001) 4284–4291. https://doi.org/10.1210/JCEM.86.9.7866.

[23] H. Tsubouchi, H. Onomura, Y. Saito, S. Yanagi, A. Miura, A. Matsuo, N. Matsumoto, M. Nakazato, Ghrelin does not influence cancer progression in a lung adenocarcinoma cell line, Endocr J. 64 (2017) S41–S46. https://doi.org/10.1507/ENDOCRJ.64.S41.

[24] G. Lentini, A. Famà, C. Biondo, N. Mohammadi, R. Galbo, G. Mancuso, D. Iannello, S. Zummo, M. Giardina, G.V. De Gaetano, G. Teti, C. Beninati, A. Midiri, Neutrophils Enhance Their Own Influx to Sites of Bacterial Infection via

Endosomal TLR-Dependent Cxcl2 Production, J Immunol. 204 (2020) 660–670. https://doi.org/10.4049/JIMMUNOL.1901039.